The Astrophysical Journal, 584:472–478, 2003 February 10


# A NEW METHOD FOR ESTIMATING WIDTHS, VELOCITIES, AND SOURCE LOCATION OF HALO CORONAL MASS EJECTIONS

G. Michałek
Astronomical Observatory of Jagiellonian University, ul. Orla 171, Krakow 30-244, Poland; michalek@oa.uj.edu.pl

and

N. Gopalswamy and S. Yashiro
Center for Solar Physics and Space Weather, Catholic University of America, Washington, DC 20064
*Received 2002 July 12; accepted 2002 October 11*

## ABSTRACT

It is well known that coronagraphic observations of halo coronal mass ejections (CMEs) are subject to projection effects. Viewing in the plane of the sky does not allow us to determine the crucial parameters that define the geoeffectiveness of CMEs, such as the space speed, width, or source location. Assuming that halo CMEs have constant velocities, are symmetric, and propagate with constant angular widths, at least in their early phase, we have developed a technique that allows us to obtain the required parameters. This technique requires measurements of sky-plane speeds and the moments of the first appearance of the halo CMEs above opposite limbs. We apply this technique to obtain the parameters of all the halo CMEs observed by the *Solar and Heliospheric Observatory* (*SOHO*) mission's Large Angle and Spectrometric Coronagraph experiment until the end of 2000. We also present a statistical summary of these derived parameters of the halo CMEs.

*Subject headings:* solar-terrestrial relations — Sun: corona — Sun: coronal mass ejections (CMEs)

## 1. INTRODUCTION

Space weather is significantly controlled by coronal mass ejections (CMEs), which can affect the Earth in different ways. CMEs originating from regions close to the central meridian of the Sun and directed toward the Earth are of immediate concern because they are likely to be geoeffective. In coronagraphic observations, halo CMEs appear as enhancements surrounding the entire occulting disk (Howard et al. 1982). Halo CMEs are routinely recorded by the highly sensitive *Solar and Heliospheric Observatory* (*SOHO*) mission's Large Angle and Spectrometric Coronagraph (LASCO). In spite of the large advantage over previous instruments, the *SOHO*/LASCO observations are still affected by projection effects because of the nature of Thomson scattering (Gopalswamy et al. 2000). Viewing in the plane of the sky does not allow us to determine the crucial parameters (space speed, width, and source location) that define the geoeffectivness of CMEs. Prediction of the arrival of CME in the vicinity of Earth is critically important in space weather investigations. On the basis of interplanetary CMEs detected by wind and the corresponding CMEs remote-sensed by *SOHO*, Gopalswamy (2002) developed and improved an empirical model to predict the arrival of CMEs at 1 AU. The critical input to this model is the initial CME speed. Better prediction could be achieved if true initial velocities are used instead of projected velocities determined from LASCO observations. Attempts have been made to estimate the projection effects on the basis of the location of the solar source by employing ad hoc assumptions of the parameters such as the CME width (Sheeley et al. 1999; Leblanc & Dulk 2001).

In the present paper we attempt to determine the space speed, width, or source location using a different technique by assuming that the CME is shaped like an ice cream cone. The method is based on the following assumptions: (1) the halo CMEs at least in the very early phase have constant velocities, (2) they are symmetric, and (3) they propagate with constant angular widths. The required inputs are the sky-plane speeds along two opposite directions and the times of first appearance above the limb in those two directions. We apply this technique to all the halo CMEs observed by *SOHO*/LASCO until the end of 2000. We compare the parameters obtained from this technique with those listed in the *SOHO*/LASCO CME catalog.

## 2. THE CONE MODEL OF CMEs

In the projection on the sky most of the CMEs (especially limb events) observed by LASCO look like cone-shaped blobs, as schematically illustrated in Figure 1. They maintain this shape during expansion through the C2 and C3 fields of view. The observed angular widths, for many limb events, remain nearly constant as a function of height (see, e.g., Webb et al. 1997). Most of them propagate with constant radial frontal speed, but many slow CMEs gradually accelerate, whereas many fast CMEs decelerate (St. Cyr et al. 2000; Sheeley et al. 1999; Gopalswamy et al. 2001; Yashiro et al. 2002). Assuming that the halo CMEs propagate with a constant velocity and angular width, we can reproduce it by the cone model with four free parameters: velocity, angular width, orientation of the central axis of the CME, and the distance of source location from the central meridian measured in the plane of the sky. These assumptions should be true at least in the beginning phase of the CME expansion. Therefore, we assume that bulk velocity of the CME is directed radially and isotropic. Similar cone models have been used before, e.g., by Howard et al. (1982), Fisher & Munro (1984), and recently by Zhao et al. (2002). In Figure 1 we show schematically basic properties of the CME model. In the projection on the symmetry plane, which intersects the ice cream cone along the central axis, it looks like a triangle represented by thick solid arrows. The central axis of our CME is represented by a thick dashed arrow. The inclination of the symmetry axis to the sky plane is $\gamma$. Each part of this cone (triangle in projection) has a constant velocity $V$. The CME with an angular width $\alpha$ is

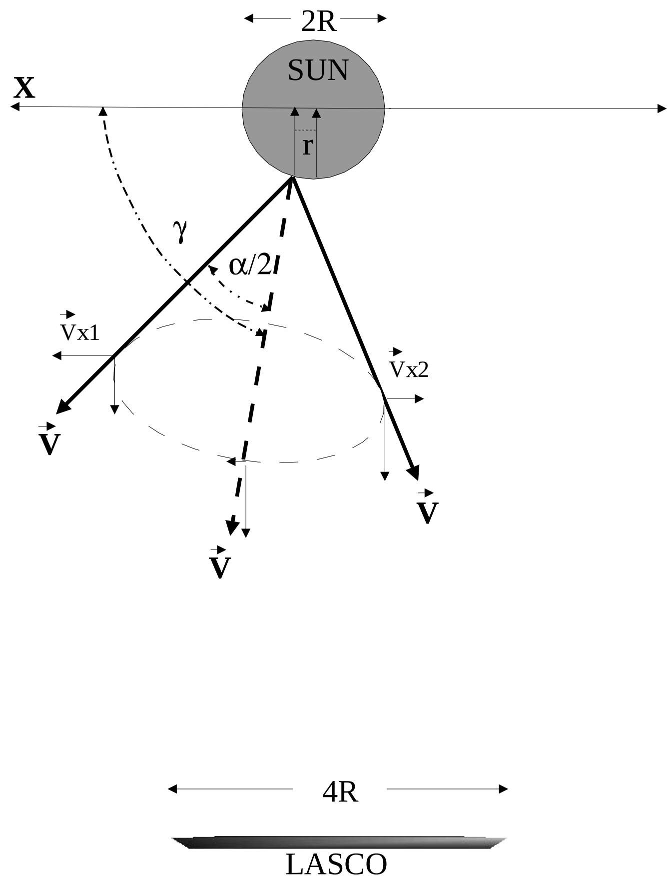


FIG. 1.—Schematic picture presenting our cone model of the halo CME. In the bottom of the picture, we see the occulting disk of the LASCO/C2 coronagraph. It should be noted that this is only a schematic picture without a real scale.

ejected from the solar surface at a distance $r$ from the central meridian. Opposite parts of CMEs have velocities $V_{x1}$ and $V_{x2}$, respectively. We note that if the CME originates exactly from the disk center, it will appear at the same time all around the occulting disk. If the source location of CME is slightly shifted ($=r$) with respect to the center of the Sun (as in Fig. 1), then the CME will first appear above the left (eastern) side of the occulting disk and finally above the right (western) side of the occulting disk. In that case, the halo CME will be asymmetric with respect to the occulting disk. This asymmetry (the difference between times when CME appears at the opposite limbs) is fundamental for our considerations.

By simple inspection we see from Figure 1 that on the left (eastern) side of the occulting disk, the CME has to travel a distance $2R - r$ with velocity $V_{x1}$ to appear in coronagraph at time $T_1$ such that

$$T_1 = \frac{(2R - r)}{V_{x1}} .$$

Similarly, the CME will appear on the right (western) side of the occulting disk after a time

$$T_2 = \frac{(2R + r)}{V_{x2}} .$$

From these equations, we determine the time difference

$$\Delta T = T_2 - T_1 = \frac{(2R + r)}{V_{x2}} - \frac{(2R - r)}{V_{x1}} . \tag{1}$$

From the geometry of the CME shown in Figure 1, we get rest of the necessary equations:

$$\cos(\gamma) = \frac{r}{R} , \tag{2}$$

$$\cos\left(\gamma - \frac{\alpha}{2}\right) = \frac{V_{x1}}{V} , \tag{3}$$

$$\cos\left(180^\circ - \gamma - \frac{\alpha}{2}\right) = \frac{V_{x2}}{V} . \tag{4}$$

We have four equations and four parameters to determine $r$, $\alpha$, $V$, and $\gamma$. The inputs $V_{x1}$, $V_{x2}$, and $\Delta T$ need to be obtained from observations. In our considerations, we use data from the *SOHO*/LASCO C2 coronagraph with a projected radius of an occulting disk approximately equal to $2R$. To reduce errors, we determine the inputs parameters from height-time plots extrapolated to the projected heliocentric distance equal to $2R$ also.

### 2.1. *Determination of Parameters Describing Halo CMEs*

Obtaining $V_{x1}$, $V_{x2}$, and $\Delta T$ from LASCO observations is not an easy task because the halo CMEs are typically very faint, and their structure is often very complicated. From LASCO observations, we obtained two height-time plots for each halo CME from our sample. The first height-time plot is for that part of the CME that appears as the first above the occulting disk. At the time of the first appearance, each CME arrives at a different height, so we extrapolated the plot to estimate the time ($T_1$) when it reaches a heliocentric distance ($=2R$) and hence obtains the velocity $V_{x1}$. The second height-time plot from the opposite limb (where the halo CME appears as last) is used to determine $T_2$ and $V_{x2}$. We illustrate this method using the example of the 1999 June 29 CME shown in Figure 2. In the first panel at the time $T_0$,

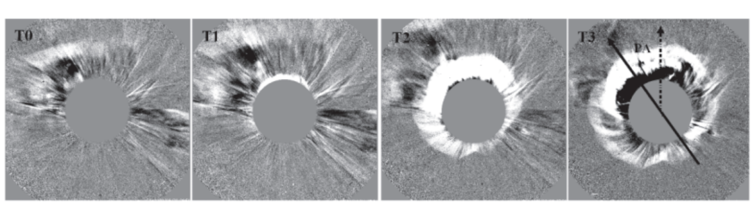


FIG. 2.—In the successive panels we present the expansion of the 1999 September 29 halo CME monitored by the LASCO/C2 coronagraph. In the last panel, the thick solid arrows present the axis along which $V_{x1}$ and $V_{x2}$ are determined. The position angle (P.A. = angle between north pole of the Sun and the part of the halo CME where $V_{x1}$ is determined) is indicated also.

we do not see any new event. In the next panel, we see that the CME appears at 07:31 UT in the northwest quadrant of the Sun. From the height-time plot, we get $T_1 = 07:19$ UT and $V_{x1} = 635$ km s$^{-1}$. In the next panel, we see that the final part of CME appears in the southwest quadrant of the Sun. From this part, we determine $T_2 = 07:34$ and $V_{x2} = 515$ km s$^{-1}$. In the fourth panel, we can see the full image of the halo CME. The thick solid arrow represents the axis along which the respective parameters are determined. The position angle (P.A. = angle between the north pole of the Sun and the part of the halo CME where $V_{x1}$ is determined) is also indicated. Hence, the time difference for this event will be $\Delta T = T_2 - T_1 = 15$ minutes. Now from equations (1), (2), (3), and (4) describing our CME model, we can determine $V = 698$ km s$^{-1}$, width $= 112°$, and parameter $r = 0.15$.

## 3. RESULTS

The height-time plots were measured for each of the halo CMEs in the LASCO CME catalog, and the results are presented in Table 1. Columns (1)–(3) are from the *SOHO*/LASCO catalog (date, time, and projected speed from LASCO observations). In columns (4)–(7), we have listed the input parameters obtained from LASCO images (P.A., $V_{x1}$, $V_{x2}$, $\Delta T$). Parameters estimated from our cone model ($r$, $\gamma$, $\alpha$, $V$) are presented in columns (8), (9), (10), and (11). A short description of the events is given in column (12). Numbers describe the quality of a given CME, with 0 for a very faint CME that cannot be measured, 1 for a faint CME for which we can measure only two points in a height-time plot, 2 for a bright CME, and finally 3 for a very bright CME. The letters F, B, and B? denote frontsided, backsided, and probably backsided halo CME, respectively. If a halo CME is too faint to generate a height-time plot at opposite limbs, we could not estimate the necessary parameters, so in column (12) we listed quality 0 without a letter designation. Similarly, we could not determine the parameters for the symmetric halo CMEs. This the case when the asymmetry in velocity is less than 10 km s$^{-1}$ or when the time difference is less than 10 minutes. For these cases we listed " Sym " in column (12). In column (13), we have listed the source location of the CME from the *GOES* X flare onset.

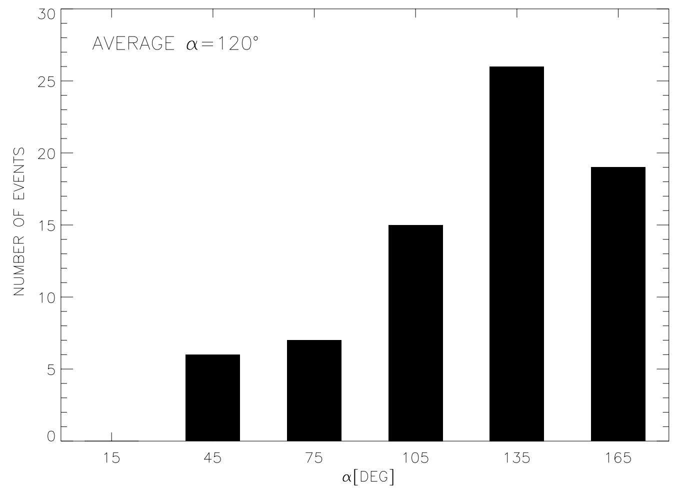


FIG. 4.—Histogram showing the distribution of $\alpha$ for the halo CMEs

### 3.1. *Properties of the Halo CMEs*

In Table 1 we have presented all the halo CMEs from 1996 August until the end of 2000. We have to note that not all halo CMEs look identical. We have to consider two types of halo CMEs. First, there are the classical full halo CMEs that appear to surround the occulting disk very fast in the LASCO/C2 field of view. Generally, they originate from a region close the disk center. Second, there are the wide limb CMEs that surround the entire occulting disk very late, often in the field of view of LASCO C3. Sometimes limb events appear as halos on account of deflections of preexisting coronal structures by the fast CME. So we have to be very careful to distinguish between a real halo CME and a limb fast event deflecting coronal material. We were able to determine the respective parameters for 72 CMEs from our sample. For reasons such as complicated or symmetric structures and faintness, it was difficult to accomplish the necessary measurements for the rest of the events from the list. In three histograms (Figs. 3, 4, and 5), we present the distribution of $V$, $\alpha$, and $\gamma$. It was noted before, e.g., by Webb et al. (1999), that halo CMEs are much faster and more energetic than typical CMEs. This is also confirmed

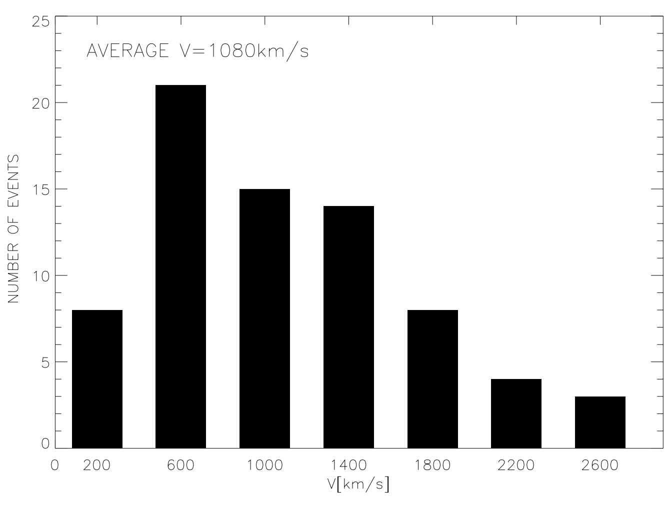


FIG. 3.—Histogram showing the distribution of $V$ for the halo CMEs

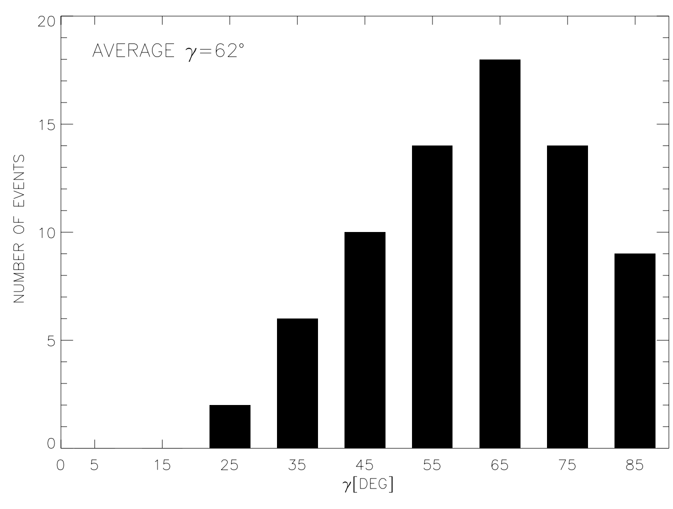


FIG. 5.—Histogram showing the distribution of $\gamma$ for the halo CMEs

TABLE 1

List of Halo CMEs

| Date (1) | Time (2) | Speed ($km\ s^{-1}$) (3) | P.A. (deg) (4) | $V_{x1}$ ($km\ s^{-1}$) (5) | $V_{x2}$ ($km\ s^{-1}$) (6) | $\Delta T$ Min (7) | $r$ ($1/R_{\odot}$) (8) | $\gamma$ (deg) (9) | $\alpha$ (deg) (10) | $V$ ($km\ s^{-1}$) (11) | Type (12) | Flare (13) |
|---|---|---|---|---|---|---|---|---|---|---|---|---|
| 1996 Aug 16 ... | 14:14:06 | 364 | 96 | 405 | 220 | 62 | 0.17 | 80 | 59 | 660 | 1.0, B? | ... |
| 1996 Nov 7..... | 23:20:05 | 497 | 114 | 412 | 361 | 18 | 0.16 | 80 | 133 | 429 | 1.0, B? | ... |
| 1996 Dec 2...... | 15:35:05 | 538 | 270 | 392 | 232 | 79 | 0.47 | 61 | 128 | 392 | 1.5, B? | ... |
| 1997 Jan 6 ...... | 15:10:42 | 136 | 182 | 100 | 85 | 75 | 0.13 | 82 | 105 | 117 | 0.5, F | S20W03 |
| 1997 Feb 7...... | 00:30:05 | 490 | 260 | 297 | 160 | 140 | 0.51 | 58 | 121 | 297 | 1.5, F | S20W04 |
| 1997 Apr 7 ..... | 14:27:44 | 875 | 126 | 956 | 551 | 23 | 0.42 | 65 | 139 | 954 | 2.0, F | S30E19 |
| 1997 May 12... | 06:30:09 | 464 | ... | ... | ... | ... | ... | ... | ... | ... | Sym | N21W08 |
| 1997 Jul 30 ..... | 04:45:47 | 104 | 276 | 94 | 85 | 81 | 0.25 | 75 | 146 | 95 | 1.0, B | ... |
| 1997 Aug 30 ... | 01:30:35 | 405 | 65 | 397 | 163 | 103 | 0.21 | 78 | 56 | 590 | 1.0, F | N30E17 |
| 1997 Sep 28 .... | 01:08:33 | 359 | 66 | 210 | 118 | 169 | 0.53 | 57 | 131 | 212 | 3.0, B | ... |
| 1997 Oct 21 .... | 18:03:45 | 523 | 30 | 527 | 356 | 35 | 0.24 | 75 | 103 | 580 | 1.0, F | N20E12 |
| 1997 Oct 23 .... | 11:26:50 | 503 | ... | ... | ... | ... | ... | ... | ... | ... | 0.0, B | ... |
| 1997 Nov 4..... | 06:10:05 | 755 | ... | ... | ... | ... | ... | ... | ... | ... | Sym | S14W33 |
| 1997 Nov 6..... | 12:10:41 | 1556 | 261 | 1524 | 765 | 34 | 0.82 | 34 | 153 | 2059 | 1.5, F | S18W63 |
| 1997 Nov 17... | 08:27:05 | 611 | ... | ... | ... | ... | ... | ... | ... | ... | Sym | ... |
| 1997 Dec 18.... | 23:47:31 | 417 | 68 | 321 | 270 | 40 | 0.36 | 68 | 158 | 325 | 2.5, B | ... |
| 1998 Jan 2 ...... | 23:28:20 | 438 | 258 | 281 | 142 | 197 | 0.93 | 20 | 165 | 602 | 2.0, B? | ... |
| 1998 Jan 17 .... | 04:09:20 | 350 | ... | ... | ... | ... | ... | ... | ... | ... | 0.0, B | ... |
| 1998 Jan 21 .... | 06:37:25 | 361 | 176 | 387 | 265 | 80 | 0.71 | 44 | 159 | 468 | 0.5, F | S57E19 |
| 1998 Jan 25 .... | 15:26:34 | 693 | 36 | 471 | 216 | 98 | 0.50 | 60 | 114 | 471 | 1.0, F | N24E27 |
| 1998 Mar 29 ... | 03:48:00 | 1794 | ... | ... | ... | ... | ... | ... | ... | ... | 0.0, B? | ... |
| 1998 Mar 31 ... | 06:12:02 | 1992 | 167 | 1733 | 502 | 41 | 0.26 | 74 | 53 | 2591 | 3.0, B? | ... |
| 1998 Apr 23.... | 06:55:20 | 1618 | 113 | 1744 | 945 | 21 | 0.51 | 59 | 126 | 1744 | 3.0, F | ... |
| 1998 Apr 27.... | 08:56:06 | 1434 | ... | ... | ... | ... | ... | ... | ... | ... | 0.0, F | S16E50 |
| 1998 Apr 29.... | 16:58:54 | 1374 | 16 | 1071 | 794 | 17 | 0.26 | 74 | 111 | 1134 | 2.0, F | S17E20 |
| 1998 May 1 .... | 23:40:09 | 585 | 142 | 623 | 367 | 31 | 0.1 | 84 | 40 | 1427 | 2.0, F | S18W05 |
| 1998 May 2 .... | 05:31:56 | 542 | 143 | 661 | 426 | 23 | 0.1 | 85 | 39 | 1612 | 2.0, F | S20W17 |
| 1998 May 2 .... | 14:06:12 | 938 | ... | ... | ... | ... | ... | ... | ... | ... | Sym | S15W15 |
| 1998 Jun 4 ...... | 02:04:45 | 1802 | ... | ... | ... | ... | ... | ... | ... | ... | 0.0, B | ... |
| 1998 Jun 5 ...... | 12:01:53 | 320 | 223 | 170 | 109 | 215 | 0.78 | 39 | 159 | 227 | 1.0, F | S23E43 |
| 1998 Jun 7 ...... | 09:32:08 | 794 | 114 | 1117 | 834 | 17 | 0.4 | 66 | 143 | 1122 | 2.0, B | ... |
| 1998 Jun 20 .... | 18:20:37 | 964 | 153 | 964 | 481 | 54 | 0.8 | 35 | 153 | 1285 | 2.0, B? | ... |
| 1998 Oct 24 .... | 02:18:05 | 452 | 116 | 404 | 377 | 32 | 0.46 | 62 | 172 | 441 | 1.5, B? | ... |
| 1998 Nov 4..... | 04:54:07 | 527 | 0.0 | 390 | 158 | 114 | 0.25 | 75 | 62 | 541 | 1.5, F | N17W01 |
| 1998 Nov 5..... | 02:24:56 | 577 | 288 | 395 | 267 | 42 | 0.18 | 79 | 88 | 482 | 1.0, F | N19W10 |
| 1998 Nov 5..... | 20:58:59 | 1124 | 305 | 1092 | 378 | 55 | 0.35 | 69 | 75 | 1283 | 3.0, F | N22W18 |
| 1998 Nov 24 ... | 02:30:05 | 1744 | 224 | 1856 | 628 | 43 | 0.88 | 27 | 153 | 2655 | 3.0, F | S30W81 |
| 1998 Nov 26 ... | 03:42:05 | 488 | ... | ... | ... | ... | ... | ... | ... | ... | 0.0 | ... |
| 1998 Dec 18.... | 18:21:50 | 1745 | 40 | 1758 | 532 | 50 | 0.68 | 47 | 120 | 1792 | 2.0, F | N19E64 |
| 1999 Apr 4 ..... | 04:30:07 | 1178 | ... | ... | ... | ... | ... | ... | ... | ... | 0.0, F | N18E72 |
| 1999 Apr 24.... | 13:31:15 | 1495 | 307 | 1259 | 502 | 45 | 0.52 | 58 | 110 | 1261 | 2.0, B | ... |
| 1999 May 3 .... | 06:06:05 | 1584 | 50 | 1392 | 345 | 61 | 0.61 | 51 | 110 | 1369 | 2.0, F | N15E32 |
| 1999 May 10... | 05:50:05 | 920 | 80 | 1080 | 513 | 33 | 0.27 | 74 | 76 | 1333 | 1.5, F | N16E19 |
| 1999 May 27... | 11:06:05 | 1691 | 311 | 1700 | 623 | 42 | 0.71 | 44 | 130 | 1821 | 1.5, B | ... |
| 1999 Jun 1 ...... | 19:37:35 | 1772 | 351 | 1792 | 662 | 32 | 0.40 | 65 | 88 | 1902 | 1.5, B | ... |
| 1999 Jun 4 ...... | 00:50:06 | 803 | 8 | 936 | 475 | 38 | 0.37 | 68 | 101 | 980 | 1.5, B? | ... |
| 1999 Jun 8 ...... | 21:50:05 | 726 | 10 | 755 | 690 | 19 | 0.49 | 60 | 170 | 834 | 1.5, F | N30E03 |
| 1999 Jun 12 .... | 21:26:08 | 465 | ... | ... | ... | ... | ... | ... | ... | ... | Sym | N22E37 |
| 1999 Jun 22 .... | 18:54:05 | 1133 | ... | ... | ... | ... | ... | ... | ... | ... | 0.0, F | N22E37 |
| 1999 Jun 23 .... | 06:06:05 | 450 | ... | ... | ... | ... | ... | ... | ... | ... | Sym | S10E71 |
| 1999 Jun 23 .... | 07:31:24 | 1006 | ... | ... | ... | ... | ... | ... | ... | ... | Sym | S12E78 |
| 1999 Jun 24 .... | 13:31:24 | 975 | ... | ... | ... | ... | ... | ... | ... | ... | 0.0, F | N29E13 |
| 1999 Jun 26 .... | 07:31:25 | 558 | 0 | 584 | 419 | 21 | 0.11 | 83 | 67 | 909 | 1.0, F | N25E00 |
| 1999 Jun 28 .... | 12:06:07 | 560 | 364 | 549 | 297 | 77 | 0.67 | 47 | 143 | 603 | 1.0, F | S27E55 |
| 1999 Jun 28 .... | 21:30:08 | 1083 | ... | ... | ... | ... | ... | ... | ... | ... | 0.0, F | S25E49 |
| 1999 Jun 29 .... | 05:54:06 | 589 | ... | ... | ... | ... | ... | ... | ... | ... | 0.0 | ... |
| 1999 Jun 29 .... | 07:31:26 | 634 | 10 | 635 | 515 | 15 | 0.15 | 81 | 112 | 698 | 2.0, F | N18E07 |
| 1999 Jun 29 .... | 18:54:07 | 438 | ... | ... | ... | ... | ... | ... | ... | ... | 0.0, F | S14E01 |
| 1999 Jun 30 .... | 04:30:05 | 1049 | ... | ... | ... | ... | ... | ... | ... | ... | 0.0 | ... |
| 1999 Jun 30 .... | 11:54:07 | 627 | 193 | 588 | 424 | 23 | 0.16 | 80 | 92 | 705 | 1.0, F | S15E00 |
| 1999 Jun 30 .... | 13:31:25 | 514 | ... | ... | ... | ... | ... | ... | ... | ... | 0.0 | ... |
| 1999 Jul 6 ....... | 17:06:05 | 899 | 350 | 1000 | 489 | 39 | 0.41 | 65 | 105 | 1026 | 1.0, B | ... |
| 1999 Jul 19 ..... | 03:06:05 | 509 | ... | ... | ... | ... | ... | ... | ... | ... | 0.0, F | N15W13 |

TABLE 1—*Continued*

| Date (1) | Time (2) | Speed (km s$^{-1}$) (3) | P.A. (deg) (4) | $V_{x1}$ (km s$^{-1}$) (5) | $V_{x2}$ (km s$^{-1}$) (6) | $\Delta T$ Min (7) | $r$ ($1/R_\odot$) (8) | $\gamma$ (deg) (9) | $\alpha$ (deg) (10) | $V$ (km s$^{-1}$) (11) | Type (12) | Flare (13) |
|---|---|---|---|---|---|---|---|---|---|---|---|---|
| 1999 Jul 25 | 13:31:21 | 1389 | 306 | 1342 | 348 | 82 | 0.76 | 40 | 127 | 1466 | 2.0, F | N29W81 |
| 1999 Jul 28 | 05:30:05 | 457 | ... | ... | ... | ... | ... | ... | ... | ... | 0.0, F | S15E00 |
| 1999 Jul 28 | 09:06:05 | 456 | ... | ... | ... | ... | ... | ... | ... | ... | 0.0, F | S15E04 |
| 1999 Aug 7 | 23:50:05 | 219 | ... | ... | ... | ... | ... | ... | ... | ... | 0.0, F | S14E47 |
| 1999 Aug 9 | 03:26:05 | 369 | ... | ... | ... | ... | ... | ... | ... | ... | 0.0, F | S29W11 |
| 1999 Oct 14 | 09:26:05 | 1250 | 63 | 1362 | 830 | 33 | 0.82 | 34 | 157 | 1899 | 2.0, F | N15E40 |
| 1999 Dec 6 | 09:30:08 | 653 | 154 | 680 | 551 | 21 | 0.33 | 70 | 147 | 682 | 1.0, B? | ... |
| 1999 Dec 12 | 08:30:05 | 720 | 198 | 1118 | 797 | 21 | 0.50 | 59 | 147 | 1151 | 1.0, B | ... |
| 1999 Dec 20 | 18:06:05 | 1237 | 15 | 1237 | 783 | 23 | 0.28 | 73 | 74 | 2242 | 2.0, B | ... |
| 1999 Dec 22 | 02:30:05 | 482 | 14 | 753 | 525 | 42 | 0.75 | 40 | 162 | 984 | 1.5, F | N10E30 |
| 1999 Dec 22 | 19:31:22 | 605 | 24 | 605 | 515 | 44 | 0.65 | 69 | 141 | 1042 | 1.5, F | N24E19 |
| 2000 Jan 14 | 10:54:34 | 229 | ... | ... | ... | ... | ... | ... | ... | ... | 0.0, B | ... |
| 2000 Jan 18 | 17:54:05 | 739 | ... | ... | ... | ... | ... | ... | ... | ... | 0.0, F | S19E11 |
| 2000 Jan 25 | 23:54:06 | 222 | ... | ... | ... | ... | ... | ... | ... | ... | 0.0 | ... |
| 2000 Jan 27 | 19:31:17 | 828 | ... | ... | ... | ... | ... | ... | ... | ... | 0.0, F | S09E71 |
| 2000 Jan 28 | 20:12:41 | 1177 | ... | ... | ... | ... | ... | ... | ... | ... | 0.0, F | S31W17 |
| 2000 Feb 3 | 12:30:05 | 735 | ... | ... | ... | ... | ... | ... | ... | ... | 0.0, B | ... |
| 2000 Feb 8 | 09:30:05 | 1079 | 55 | 938 | 732 | 28 | 0.63 | 50 | 162 | 1091 | 2.0, F | N25E26 |
| 2000 Feb 9 | 19:54:17 | 910 | 218 | 1124 | 693 | 25 | 0.44 | 63 | 128 | 1125 | 1.5, F | S17W40 |
| 2000 Feb 11 | 21:08:06 | 498 | ... | ... | ... | ... | ... | ... | ... | ... | 0.0 | ... |
| 2000 Feb 12 | 04:31:20 | 1107 | ... | ... | ... | ... | ... | ... | ... | ... | 0.0, F | N26W23 |
| 2000 Feb 17 | 20:06:05 | 600 | 196 | 660 | 540 | 23 | 0.39 | 67 | 152 | 668 | 2.0, F | S27W10 |
| 2000 Feb 28 | 10:54:05 | 404 | 279 | 466 | 370 | 43 | 0.3 | 72 | 132 | 475 | 2.0, B? | ... |
| 2000 Mar 1 | 03:30:05 | 529 | 217 | 628 | 488 | 38 | 0.64 | 49 | 162 | 737 | 2.0, B? | ... |
| 2000 Mar 3 | 05:30:07 | 793 | ... | ... | ... | ... | ... | ... | ... | ... | 0.0, F | S14W62 |
| 2000 Mar 29 | 10:54:30 | 949 | ... | ... | ... | ... | ... | ... | ... | ... | 0.0, B | ... |
| 2000 Apr 4 | 16:32:37 | 1188 | 304 | 1281 | 641 | 40 | 0.79 | 37 | 151 | 1645 | 2.0, F | N16W66 |
| 2000 Apr 10 | 00:30:05 | 383 | ... | ... | ... | ... | ... | ... | ... | ... | 0.0, F | S14W01 |
| 2000 Apr 23 | 12:54:05 | 1187 | 279 | 1309 | 533 | 46 | 0.65 | 49 | 127 | 1351 | 3.0, B | ... |
| 2000 May 3 | 02:06:05 | 693 | ... | ... | ... | ... | ... | ... | ... | ... | Sym, B | ... |
| 2000 May 5 | 15:50:05 | 1594 | 269 | 1624 | 570 | 50 | 0.85 | 32 | 146 | 2154 | 2.0, F | S16W84 |
| 2000 May 12 | 23:26:05 | 2604 | 63 | 2056 | 699 | 36 | 0.62 | 51 | 116 | 2072 | 2.0, B? | ... |
| 2000 May 28 | 11:06:05 | 572 | ... | ... | ... | ... | ... | ... | ... | ... | 0.0, B? | ... |
| 2000 Jun 2 | 10:30:25 | 442 | ... | ... | ... | ... | ... | ... | ... | ... | 0.0, F | N10E23 |
| 2000 Jun 6 | 15:54:05 | 1108 | 6 | 1024 | 870 | 12 | 0.32 | 71 | 152 | 1028 | 2.5, F | N21E15 |
| 2000 Jun 7 | 16:30:05 | 842 | ... | ... | ... | ... | ... | ... | ... | ... | 0.0, F | N20E02 |
| 2000 Jun 10 | 17:08:05 | 1108 | 306 | 1376 | 710 | 32 | 0.64 | 50 | 138 | 1460 | 2.5, F | N22W37 |
| 2000 Jul 7 | 10:26:05 | 453 | 198 | 311 | 239 | 59 | 0.42 | 65 | 147 | 315 | 1.5, B? | ... |
| 2000 Jul 11 | 13:27:23 | 1078 | 51 | 1453 | 1093 | 18 | 0.68 | 47 | 162 | 1753 | 2.0, F | N18E27 |
| 2000 Jul 14 | 10:54:07 | 1674 | ... | ... | ... | ... | ... | ... | ... | ... | 0.0, F | N22E07 |
| 2000 Jul 27 | 19:54:06 | 905 | ... | ... | ... | ... | ... | ... | ... | ... | 0.0, F | N10E07 |
| 2000 Aug 9 | 16:30:05 | 702 | ... | ... | ... | ... | ... | ... | ... | ... | 0.0, F | N11W09 |
| 2000 Sep 12 | 11:54:05 | 1550 | 216 | 1250 | 966 | 18 | 0.58 | 54 | 159 | 1385 | 2.0, F | S12W18 |
| 2000 Sep 12 | 17:30:05 | 1053 | 47 | 1329 | 681 | 27 | 0.39 | 66 | 106 | 1366 | 2.0, B? | ... |
| 2000 Sep 15 | 15:26:05 | 481 | ... | ... | ... | ... | ... | ... | ... | ... | 0.0, F | N14E02 |
| 2000 Sep 15 | 21:50:07 | 257 | ... | ... | ... | ... | ... | ... | ... | ... | 0.0, F | N14E01 |
| 2000 Sep 16 | 05:18:14 | 1251 | 21 | 1256 | 946 | 12 | 0.27 | 74 | 126 | 1278 | 2.0, F | N14E04 |
| 2000 Sep 25 | 02:50:05 | 587 | ... | ... | ... | ... | ... | ... | ... | ... | 0.0, F | N15W28 |
| 2000 Oct 2 | 03:50:05 | 525 | 144 | 577 | 381 | 42 | 0.41 | 65 | 131 | 578 | 1.0, F | S08E05 |
| 2000 Oct 2 | 20:26:05 | 569 | ... | ... | ... | ... | ... | ... | ... | ... | 0.0, F | S08E05 |
| 2000 Oct 9 | 23:50:05 | 798 | ... | ... | ... | ... | ... | ... | ... | ... | 0.0, F | N02W18 |
| 2000 Nov 1 | 16:26:08 | 801 | ... | ... | ... | ... | ... | ... | ... | ... | 0.0, F | S17E39 |
| 2000 Nov 3 | 18:26:06 | 291 | ... | ... | ... | ... | ... | ... | ... | ... | 0.0, F | N02W02 |
| 2000 Nov 8 | 04:50:23 | 474 | 236 | 622 | 294 | 77 | 0.6 | 53 | 128 | 634 | 1.0, F | N10W77 |
| 2000 Nov 8 | 23:06:05 | 1345 | ... | ... | ... | ... | ... | ... | ... | ... | 0.0, F | N05W75 |
| 2000 Nov 15 | 23:54:05 | 826 | ... | ... | ... | ... | ... | ... | ... | ... | 0.0, B | ... |
| 2000 Nov 23 | 06:06:05 | 492 | 230 | 450 | 334 | 48 | 0.49 | 60 | 150 | 466 | 1.0, F | S22W33 |
| 2000 Nov 24 | 05:30:05 | 1074 | 352 | 996 | 734 | 21 | 0.45 | 62 | 147 | 1013 | 1.5, F | N22W02 |
| 2000 Nov 24 | 15:30:05 | 1245 | 324 | 1396 | 841 | 17 | 0.26 | 74 | 96 | 1556 | 3.0, F | N22W07 |
| 2000 Nov 24 | 22:06:05 | 1005 | 312 | 1105 | 575 | 37 | 0.56 | 55 | 130 | 1122 | 2.0, F | N21W14 |
| 2000 Nov 25 | 01:31:58 | 2519 | 75 | 2434 | 724 | 34 | 0.54 | 57 | 100 | 2452 | 2.0, F | N07E50 |
| 2000 Nov 25 | 09:30:17 | 675 | ... | ... | ... | ... | ... | ... | ... | ... | 0.0, B? | ... |
| 2000 Nov 25 | 19:31:57 | 671 | ... | ... | ... | ... | ... | ... | ... | ... | 0.0, F | N20W23 |
| 2000 Nov 26 | 17:06:05 | 1026 | 283 | 1240 | 785 | 25 | 0.58 | 54 | 144 | 1303 | 2.0, F | N18W38 |

TABLE 1—*Continued*

| Date (1) | Time (2) | Speed (km s$^{-1}$) (3) | P.A. (deg) (4) | $V_{x1}$ (km s$^{-1}$) (5) | $V_{x2}$ (km s$^{-1}$) (6) | $\Delta T$ Min (7) | $r$ ($1/R_\odot$) (8) | $\gamma$ (deg) (9) | $\alpha$ (deg) (10) | $V$ (km s$^{-1}$) (11) | Type (12) | Flare (13) |
|---|---|---|---|---|---|---|---|---|---|---|---|---|
| 2000 Dec 6...... | 17:26:05 | 413 | ... | ... | ... | ... | ... | ... | ... | ... | Sym, B | ... |
| 2000 Dec 18.... | 11:50:05 | 510 | ... | ... | ... | ... | ... | ... | ... | ... | 0.0, F | N14E03 |
| 2000 Dec 28.... | 12:06:05 | 930 | ... | ... | ... | ... | ... | ... | ... | ... | Sym, B | ... |

by our results. The average width of halo CMEs is approximately equal to 120° (more than 2 times larger than the average value obtained from the *SOHO*/LASCO catalog; Yashiro et al. 2002). The most narrow CME has its width equal to 40°, and the widest one has a cone angle as large as 172°. The average speed of the halo CMEs is 1080 km s$^{-1}$ (about 2 times larger than that from the *SOHO*/LASCO catalog). The slowest one had its speed equal to 95 km s$^{-1}$, while the fastest one had its speed equal to 2590 km s$^{-1}$. Figure 5 shows that the halo CMEs originate close to the Sun center (with $\gamma \geq 60°$) with maximum of distribution around $\gamma = 65°$. We have to remember that we have excluded the symmetric halos, which start exactly from the Sun center. If we include them, then the maximum of $\gamma$ distribution would be shifted to the central meridian. In Figure 6 we present the sky-plane speeds against corrected (true) velocities. The solid line represents the linear fit to the data points. The inclination of the linear fit suggests that the projection effect increases slightly with the speed of the CMEs. It is clear that the projection effect is important, and on the average, the corrected speeds are 20% larger than the velocities measured in the plane of the sky.

## 4. SUMMARY

In this paper we have presented a new method for estimating the crucial parameters that determine the geoeffectiveness of the halo CMEs. The crucial point of this method is the time difference between the appearances of the halo at two opposite position angles. We applied this method to all the halo CMEs listed in the *SOHO*/LASCO catalog until the end of 2000. We were able to determine the true velocity, width, and source location for 72 CMEs from our sample. Unfortunately, 58 events were either symmetric or too faint to measure. These results suggest that the halo CMEs represent a special class of CMEs that are very wide and fast. Such fast and wide CMEs are known to be associated with electron and proton acceleration by driving fast-mode MHD shocks (e.g., Cane et al. 1987; Gopalswamy et al. 2001; Gopalswamy 2002a). We point out that the simple method has several shortcomings: (1) CMEs may be accelerating, moving with constant speed, or decelerating at the beginning phase of propagation. This means that the constant velocity assumption may be invalid. (2) CMEs may expand in addition to radial motion. Then the measured sky-plane speed is a sum of the expansion speed and the projected radial speed. This would also imply that the CMEs may not be a rigid cone, as we had assumed (Gopalswamy 2002b). (3) The cone symmetry also may not hold. Many halo CMEs do not emerge over opposite limbs along a symmetrical 180°; their structure is often very complicated. Unfortunately, beautiful events similar to the one presented in Figure 2 are sporadic. It is very difficult to estimate how reliable our basic assumptions (CMEs have constant velocities and constant angular width and are symmetric) are for a given CME. Each of these assumptions may be true for most CMEs but not necessarily for a particular CME. Nevertheless, there are no available data to modify the model. For our consideration, we chose only bright halo CMEs with large differences in appearance time above opposite limbs. There is still a possibility that the determined parameters for a particular halo CME (for CMEs, which completely breaks our basic assumptions) may be wrong. The "exotic" events, if they exist in our sample at all, should not affect our results. All these limits can be overcome by stereoscopic observations. Unfortunately, at the present time they are not available yet. It is necessary to improve the model to get a better fit to the observations. The first step would be to include acceleration and expansion of CMEs. We have to note that it may be surprising that the average corrected speeds are only 20% greater than the sky-plane speeds. But we have to remember that halo CMEs originating close to the Sun center, subjected to the largest projection effects, are not included in our results. They are symmetric in LASCO observations and cannot be considered using our method.

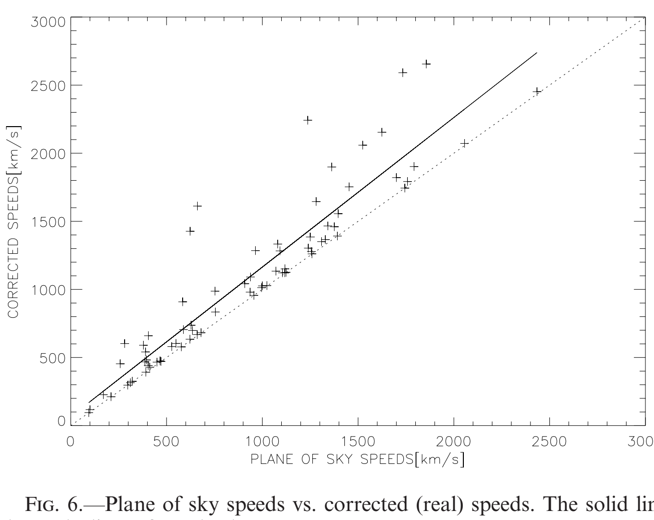


FIG. 6.—Plane of sky speeds vs. corrected (real) speeds. The solid line shows the linear fit to the data.

This paper was written while Grzegorz Michalek was working at the Center for Solar Physics and Space Weather, Catholic University of America, Washington, DC. In this paper we used data from the *SOHO*/LASCO CME catalog. This CME catalog is generated and maintained by the Center for Solar Physics and Space Weather, Catholic University of America, in cooperation with the Naval Research Laboratory and NASA. *SOHO* is a project of international cooperation between ESA and NASA. Work done by Grzegorz Michalek was partly supported by *Komitet Badań Naukowych* through grant PB 258/P03/99/17.

REFERENCES

Cane, H. V., et al. 1987, J. Geophys. Res., 92, 9869
Fisher, R. R., & Munro, R. H. 1984, ApJ, 280, 873
Gopalswamy, N. 2002a, ApJ, 572, L103
———. 2002b, in COSPAR Colloq. Ser. 12, Space Weather Study Using Multipoint Techniques, ed L.-H. Lyu (New York: Pergamon), 39
———. 2000, Geophys. Res. Lett., 27, 1427
———. 2001, J. Geophys. Res., 106, 292907
Howard, R. A., et al. 1982, ApJ, 263, L101
Leblanc, Y., & Dulk, G. A. 2001, J. Geophys. Res., 106, 25301
Sheeley, N. R., Jr., Walters, J. H., Wang, Y.-M., & Howard, R. A. 1999, J. Geophys. Res., 104, 24739
St. Cyr, O. C., et al. 2000, J. Geophys. Res., 105, 18169
Webb, D. F., et al. 1997, J. Geophys. Res., 102, 24161
———. 1999, BAAS, 31, 853
Yashiro, S., et al. 2002, BAAS, 34, 37.04
Zhao, X. P., Plunkett, S. P., & Liu, W. 2002, J. Geophys. Res., 107(A8), 10.1029/2001JA009143